Independently Regulated Multi-compartment Neuropeptide Release from a Clock Neuron Controls Circadian Behavior

Markus K. Klose[a], Marcel P. Bruchez[b,c,d], David L. Deitcher[e], and Edwin S. Levitan[a]*

[a]Department of Pharmacology and Chemical Biology, University of Pittsburgh, Pittsburgh, PA 15261; [b]Molecular Biosensor and Imaging Center, Carnegie Mellon University, Pittsburgh, PA 15213; [b]Department of Chemistry, Carnegie Mellon University, Pittsburgh, PA 15213; and [d]Department of Biological Sciences, Carnegie Mellon University, Pittsburgh, PA 15213; [e]Department of Neurobiology and Behavior, Cornell University, Ithaca, NY 14853

*Correspondence to: ELevitan@Pitt.edu

Neuropeptides control many behaviors, including circadian rhythms. However, because monitoring neuropeptide release in the brain is challenging, analysis of peptidergic circuits often has relied on monitoring surrogates in the soma based on the paradigm that synaptic transmission is mediated exclusively by Ca^{2+} influx induced by propagating action potentials. Here live imaging demonstrates that neuropeptide release by *Drosophila* small ventrolateral (s-LNv) clock neurons does not conform to this paradigm. First, neuropeptide release from terminals peaks hours after sunrise, which was not evident from electrical and Ca^{2+} data. Second, inconsistent with global release by propagating action potentials, release from terminals is preceded by hours by release from the soma, a compartment not usually considered in peptidergic transmission. The timing of release from the two neuronal compartments reflects different mechanisms: terminals require Ca^{2+} influx, as expected with coupling to electrical activity, while somatic release is based on intracellular IP_3 signaling. Upon cell specific disruption of the somatic mechanism, daily neuropeptide release from terminals remains rhythmic and the period of daily locomotor activity is unaffected, but behavioral rhythmicity is reduced. Thus, rhythmic bouts of anatomically, mechanistically and temporally distinct release from a single neuron control neuropeptide dependent features of circadian behavior.

Direct observations of neuropeptide exocytosis from central neurons cells are strikingly absent from the literature. Understanding this important mechanism for intercellular communication within neural networks in the brain relied traditionally on studies of stained fixed tissue, where loss of neuropeptide signal was assumed to demarcate release (Taghert and Nitabach, 2012; Nusbaum et al., 2017). However, this approach is only applicable when release is dramatic and relies on assuming that transport, capture and degradation of neuropeptide-containing dense-core vesicles (DCVs) do not contribute to measured changes. Therefore, recent studies have relied on measurements of somatic electrical activity and Ca^{2+} as surrogates for action potential-evoked Ca^{2+} influx at distal release sites. Interestingly, these indirect approaches have not provided a clear consensus about the timing of neuropeptide release by s-LNv and large LNv (l-LNv) clock neurons that participate in *Drosophila* circadian rhythms; the daily rhythms of the decrease in neuropeptide in the distal terminal release sites, electrical activity and cytosolic Ca^{2+} are not coincident (Park et al., 2000; Cao & Nitabach, 2008; Liang et al., 2016). Therefore, we set out to optically measure synaptic neuropeptide release in the excised intact brain.

For *Drosophila* s-LNv neurons, an early attempt at using a GFP-tagged mammalian neuropeptide was not fruitful because of genetic background effects (Kula et al., 2006). However, we found that known rhythmic changes in the native neuropeptide pigment dispersing factor (PDF) in s-LNv neuron terminals and somas (Park et al., 2000) are recapitulated by GFP-tagged *Drosophila* preproinsulin-like peptide 2 (Dilp2-GFP) (Fig. 1). Furthermore, the known absence of rhythmic changes in PDF of l-LNv neurons was also evident with Dilp2-GFP (Fig. S1). The preservation of normal function led us to use a more sensitive Dilp2-based release indicator, which employs a fluorogen activating protein (FAP) that produces fluorescence upon the opening of DCV fusion pores that mediate synaptic release of neuropeptides (Bulgari et al., 2019). Specifically, the Dilp2-FAP approach was used to measure daily rhythms in neuropeptide release.

Data from s-LNv and l-LNv terminals showed that both the duration and time of day for peak endogenous synaptic release do not fit with predictions for either cell type derived from somatic recordings of electrical activity and Ca^{2+}: s-LNv neuron synaptic

neuropeptide release peaks 3 hours after sunrise (ZT3) (Fig. 2A, B), while l-LNv neurons have a burst of synaptic release late at night (ZT23) (Fig. S2A). Interestingly, at ZT1 when endogenous release at s-LNv terminals is normally low, K^+-induced depolarization evoked ectopic release (Fig. S3). This shows that DCVs at synaptic sites of release (Yasuyama and Meinertzhagen, 2010) are present and competent for release, but must wait for electrical activity or some other cellular signal to initiate rhythmic release.

Although the soma is not usually considered to participate in physiological peptidergic transmission, FAP imaging revealed endogenous somatic neuropeptide release in a variety of identified neurons, including LNv clock (Fig. 2C) and non-clock neurons (data not shown), suggesting that somatic release may be widespread in the brain. Furthermore, s-LNv and l-LNv FAP experiments also demonstrated that daily rhythmic synaptic release is preceded hours earlier by somatic neuropeptide release (peak somatic release was at ZT23 in s-LNv neurons and at ZT18 in l-LNv neurons) (Fig. 2D and S2B). Although electrical signaling in this subset of neurons is required for normal clock circuit function and behavior (Nitabach et al., 2002), the different timing of release from terminals and the soma excludes propagating action potentials as the sole mechanism of evoking release from different sites in the same neuron.

If electrical activity does not couple release from terminals and the soma, what mechanism is responsible for somatic neuropeptide release? Recently, FAP imaging revealed that there is spontaneous neuropeptide release, which is independent of extracellular Ca^{2+} and resistant to tetanus toxin (TeTx) (Bulgari et al., 2019). However, TeTx expression comparably reduced release from both the soma and terminals of s-LNv neurons (Fig. 3 A, B). The incomplete inhibition of release from either compartment likely explains why TeTx fails to disrupt circadian behaviors mediated by the neuropeptide PDF, which is an important clock signal released by s-LNv and l-LNv neurons (Kaneko et al., 2005; Blanchardon et al., 2001). More importantly here, TeTx inhibition of release from the soma and terminals suggests that Ca^{2+} evokes timed release from both compartments.

Therefore, we tested for a role of extracellular Ca^{2+} influx by incubating the excised brain in the Ca^{2+} channel blocker Cd^{2+}. As expected, peak synaptic

neuropeptide release was inhibited. However, somatic neuropeptide release was unaffected (Fig. 4 A, B). This led us to examine the role of IP_3 (inositol trisphosphate) receptors (IP3Rs), which mediate intracellular Ca^{2+} release from the endoplasmic reticulum into the cytosol to participate in Ca^{2+} influx independent neuropeptide release at the neuromuscular junction (Shakiryanova *et al.*, 2011). First, 100 nM Xestospongin C, a blocker of IP3Rs (Gafni et al., 1997; Klose et al., 2010; James et al., 2019), was applied acutely. Strikingly, while peak endogenous neuropeptide release from terminals was unaffected, peak endogenous neuropeptide release from the soma was inhibited (Fig. 4 C, D). To independently test for a role for IP3 receptor signaling in somatic neuropeptide release, IP_3 sponge, which binds IP_3 to interfere with its second messenger function (Uchiyama *et al.*, 2002; James *et al.*, 2019), was expressed along with the FAP reporter in s-LNv clock neurons and tested for effects on neuropeptide release at times of the day when release varies in terminals and the soma (ZT23 and ZT3, Fig. 2). Consistent with the Xestospongin C results, neuropeptide release from s-LNv terminals remained rhythmic (Fig. 5A) and peak somatic release at ZT23 (Fig. 2D) was abolished (Fig. 5B). Together, these data show that different compartments of the s-LNv neuron release neuropeptides at different times of the day by engaging different mechanisms (i.e., extracellular Ca^{2+} influx for terminals and IP_3 signaling for the soma).

Transmission by the neuropeptide PDF from s-LNv neurons regulates rhythm period and promotes rhythmicity (Renn et al., 1999; Hyun et al. 2005; Choi et al., 2012; Klose et al., 2016). Because IP_3 sponge selectively ablates somatic neuropeptide release, we examined the behavior of flies expressing IP3 sponge in LNv neurons for effects on clock function and output. Importantly, expression of Dilp2-FAP in s-LNv and l-LNv neurons with the *Pdf*-Gal4 driver did not perturb circadian behavior. However, expression of UAS-*IP3 sponge* in LNv clock neurons halved the number of flies that exhibit rhythmic locomotor behavior compared to genetic controls (Fig. 5C). In contrast, no effect was observed on the period of any flies tested that maintain rhythmic behavior (Figure 5D). Thus, IP_3-sponge experiments suggest compartment-specific regulation of specific parameters of circadian behavior.

FAP imaging revealed synaptic neuropeptide release from LNv clock neurons that does not conform to predictions from previously used methods. Measuring content

could not resolve whether somatic changes were due to release or traffic and missed l-LNv rhythmic neuropeptide release likely because it is relatively modest and/or obscured by DCV capture that replenishes synaptic neuropeptide stores (Shakiryanova et al., 2006; Wong et al., 2012). Somatic Ca^{2+} was not reflective of terminals because of IP_3 signaling. Finally, somatic electrical recording cannot take into account regulation by presynaptic inputs. Thus, direct live imaging of neuropeptide release is essential for monitoring peptidergic transmission in the brain. Indeed, this approach demonstrates that that central clock neurons release neuropeptide from terminals and the soma, with each compartment operating with different mechanisms and timing. Release from s-LNv clock neuron terminals is conventional (i.e., mediated by extracellular Ca^{2+} influx), but somatic neuropeptide release is triggered by IP_3 signaling that operates in the absence of Ca^{2+} influx induced by electrical activity. Different release mechanisms allow for multi-phasic temporal control of neuropeptide release from separate compartments of the same neuron, each of which releases onto different parts of the clock circuit thereby influencing different parameters of behavior.

Materials and Methods

Flies

All flies were reared on cornmeal/agar supplemented with yeast. Male flies were collected on the day of eclosion and maintained on a 12 hour light: 12 hour dark photoperiod for physiological experiments. Flies were maintained at 25ºC. Genotypes include: UAS-*Dilp2-GFP*; *Pdf*-Gal4, UAS-*Dilp2-FAP*; *Pdf*-Gal4, UAS-*Dilp2-FAP*/UAS-*Dil2-pGFP*; *Pdf*-Gal4, UAS-*Dilp2-FAP*; UAS-*IP_3 sponge Pdf*-Gal4, UAS-*Dilp2-FAP*; UAS-*IP_3 sponge*. Expression of tetanus toxin light chain and a control mutant (Sweeney *et al.*, 1995) were induced by crosses to UAS lines (Bloomington #28838 and 28840).

Imaging

Imaging experiments were performed on adult brain explants, bathed in HL3 saline, which contained (in mM) 70 mM NaCl, 5 KCl, 1.5 $CaCl_2$, 20 $MgCl_2$, 10 $NaHCO_3$, 5 trehalose, 115 sucrose, and 5 sodium Hepes, pH 7.2. Brains were dissected in Ca^{2+}-free HL3 saline (0.5 mM EGTA in place of Ca^{2+}), then transferred to HL3 saline. To elicit

depolarization-evoked release, HL3 was modified by increasing KCl to 70 mM by substituting NaCl. Data were acquired using an Olympus Fluoview 1000 confocal microscope with a 60× 1.0 NA water immersion objective. MG-FAP was imaged with Cy5 fluorescence optics. A 478 nm laser and standard FITC optics were used for imaging GFP. Brains were placed in HL3 filled Sylgaard chambers that were pre-treated with poly-L-lysine, which acted as an adherent. Membrane impermeant MG-B-Tau (MG) was added to the bathing solution at a final concentration of 1 µM. All release measurements were acquired after 60 minutes of bathing in MG-B-Tau. Quantification of fluorescence intensity was performed with ImageJ software (https://imagej.nih.gov/ij/). For s-LNv terminal GFP content, an region of interest was drawn around the s-LNv dorsal protocerebral projection stack. l-LNv GFP terminal content was the average of 10 boutons for each hemi-segment. For s-LNv terminal release, 6-10 boutons were averaged for each measurement. s-LNv and l-LNv somata measurements are the average of 2-4 cells from each hemi-segment. Images were taken at several times points during both the day and night and all measurements were background subtracted.

Behavior

Adult flies (3-4 days old) were loaded into glass tubes and placed in DAM2 Trikinetics Activity Monitors and entrained for 7 days on 12hr:12hr light:dark schedule, then released into constant darkness for 8 days. We assessed rhythmicity by normalizing activity from DD days 2–8. We defined arrhythmic flies by rhythmicity threshold [Qp.act/Qp.sig] below 1 or a period estimate <18 hr or >30 hr. Rhythmicity and period were assessed using ShinyR software (Cichewicz and Hirsh, 2018).

Analysis

Statistical analysis and graphing were performed with Graphpad Prism software. Error bars represent Standard Error of the Mean (SEM). Statistical comparison for two experimental groups was based on Student’s t test. For multiple comparisons, one-way ANOVA was followed with Tukey’s post-test.

Chemicals

MG derivatives were synthesized as previously described (Yan et al., 2015; Perkins et al., 2018). Pharmacological agents were bath applied in recording saline at the final concentrations indicated in the text. Purchased chemicals included Xestospongin C (CAS Number: Abcam 88903-69-9) and cadmium chloride (Sigma).

References

Blanchardon E, Grima B, Klarsfeld A, et al. Defining the role of Drosophila lateral neurons in the control of circadian rhythms in motor activity and eclosion by targeted genetic ablation and PERIOD protein overexpression. Eur J Neurosci. 2001;13(5):871-888. doi:10.1046/j.0953-816x.2000.01450.x

Bulgari D, Deitcher DL, Schmidt BF, Carpenter MA, Szent-Gyorgyi C, Bruchez MP, Levitan ES. Activity-evoked and spontaneous opening of synaptic fusion pores. Proc Natl Acad Sci U S A. (2019) Aug 20;116(34):17039-17044.

Cao G, Nitabach MN. Circadian control of membrane excitability in Drosophila melanogaster lateral ventral clock neurons. J Neurosci. 2008;28(25):6493-6501. doi:10.1523/JNEUROSCI.1503-08.2008

Cichewicz K. & Hirsh J., ShinyR-DAM: A program analyzing Drosophila activity, sleep, and circadian rhythms, Commun. Biol. 1, 25 (2018)

Choi C, Cao G, Tanenhaus AK, et al. Autoreceptor control of peptide/neurotransmitter corelease from PDF neurons determines allocation of circadian activity in drosophila. Cell Rep. 2012;2(2):332-344. doi:10.1016/j.celrep.2012.06.021

Gafni J, Munsch JA, Lam TH, Catlin MC, Costa LG, Molinski TF, Pessah IN. Xestospongins: potent membrane permeable blockers of the inositol 1,4,5-trisphosphate receptor. Neuron. 1997; 19:723–733. doi: 10.1016/S0896-6273(00)80384-0.

Hyun S, Lee Y, Hong ST, et al. Drosophila GPCR Han is a receptor for the circadian clock neuropeptide PDF. Neuron. 2005;48(2):267-278. doi:10.1016/j.neuron.2005.08.025

James TD, Zwiefelhofer DJ, Frank CA. Maintenance of homeostatic plasticity at the

Drosophila neuromuscular synapse requires continuous IP3-directed signaling. Elife. 2019;8:e39643. Published 2019 Jun 10. doi:10.7554/eLife.39643

Kaneko M, Park JH, Cheng Y, Hardin PE, Hall JC. Disruption of synaptic transmission or clock-gene-product oscillations in circadian pacemaker cells of Drosophila cause abnormal behavioral rhythms. J Neurobiol. 2000;43(3):207-233. doi:10.1002/(sici)1097-4695(20000605)43:3<207::aid-neu1>3.0.co;2-0

Klose MK, Dason JS, Atwood HL, Boulianne GL, Mercier AJ. Peptide-induced modulation of synaptic transmission and escape response in Drosophila requires two G-protein-coupled receptors. J Neurosci. 2010;30(44):14724-14734. doi:10.1523/JNEUROSCI.3612-10.2010

Klose M, Duvall L, Li W, et al. Functional PDF Signaling in the Drosophila Circadian Neural Circuit Is Gated by Ral A-Dependent Modulation. Neuron. 2016;90(4):781-794. doi:10.1016/j.neuron.2016.04.002

Kula E, Levitan ES, Pyza E, Rosbash M. PDF cycling in the dorsal protocerebrum of the Drosophila brain is not necessary for circadian clock function. J Biol Rhythms. 2006; 21(2):104-117. doi: 10.1177/0748730405285715

Liang X, Holy TE, Taghert PH. Synchronous Drosophila circadian pacemakers display nonsynchronous Ca^{2+} rhythms in vivo. Science. 2016;351(6276):976-981. doi:10.1126/science.aad3997

Nitabach MN, Blau J, Holmes TC. Electrical silencing of Drosophila pacemaker neurons stops the free-running circadian clock. Cell. 2002;109(4):485-495. doi:10.1016/s0092-8674(02)00737-7

Nusbaum MP, Blitz DM, Marder E, Functional consequences of neuropeptide and small-molecule co-transmission. Nat. Rev. Neurosci. 18, 389–403 (2017).

Park JH, Helfrich-Förster C, Lee G, Liu L, Rosbash M, Hall JC. Differential regulation of circadian pacemaker output by separate clock genes in Drosophila. Proc Natl Acad Sci U S A. 2000;97(7):3608-3613. doi:10.1073/pnas.070036197

Perkins, LA, Fisher, G, Naganbabu, M, Schmidt, B, Mun, F, and Bruchez, MP High-content Surface and Total expression siRNA Kinase Library Screen with VX-809 Treatment Reveals Synergistic Kinase Targets that Enhance F508del-CFTR Rescue. Mol Pharm. 2018 Mar 5;15(3):759-767. doi: 10.1021/acs.molpharmaceut.7b00928.

Renn SC, Park JH, Rosbash M, Hall JC, Taghert PH. A pdf neuropeptide gene mutation and ablation of PDF neurons each cause severe abnormalities of behavioral circadian rhythms in Drosophila [published correction appears in Cell 2000 Mar 31;101(1):following 113]. Cell. 1999;99(7):791-802. doi:10.1016/s0092-8674(00)81676-1

Shakiryanova D, Zettel GM, Gu T, Hewes RS, Levitan ES. Synaptic neuropeptide release induced by octopamine without Ca2+ entry into the nerve terminal. Proc Natl Acad Sci U S A. 2011;108(11):4477-81. doi: 10.1073/pnas.1017837108.

Shakiryanova D, Tully A, Levitan ES. Activity-dependent synaptic capture of transiting peptidergic vesicles. Nat Neurosci. 2006;9(7):896-900. doi: 10.1038/nn1719.

Sweeney ST, Broadie K, Keane J, Niemann H, O'Kane CJ. Targeted expression of tetanus toxin light chain in Drosophila specifically eliminates synaptic transmission and causes behavioral defects. Neuron 14, 341–351 (1995).

Taghert, PH, Nitabach MP, Peptide neuromodulation in invertebrate model sys- tems. Neuron 76, 82–97 (2012).

Uchiyama T, Yoshikawa F, Hishida A, Furuichi T, Mikoshiba K. A novel recombinant

hyperaffinity inositol 1,4,5-trisphosphate (IP(3)) absorbent traps IP(3), resulting in specific inhibition of IP(3)-mediated calcium signaling. J Biol Chem. 2002;277(10):8106-13. doi: 10.1074/jbc.M108337200.

Wong MY, Zhou C, Shakiryanova D, Lloyd TE, Deitcher DL, Levitan ES. Neuropeptide delivery to synapses by long-range vesicle circulation and sporadic capture. Cell. 2012;148(5):1029-1038. doi:10.1016/j.cell.2011.12.036

Yan Q *et al.* Near-instant surface-selective fluorogenic protein quantification using sulfonated triarylmethane dyes and fluorogen activating proteins. Org Biomol Chem. 2015; 13(7): 2078–2086. doi: 10.1039/c4ob02309a

Yasuyama K, Meinertzhagen IA. Synaptic connections of PDF-immunoreactive lateral neurons projecting to the dorsal protocerebrum of Drosophila melanogaster. J Comp Neurol. 2010;518(3):292-304. doi:10.1002/cne.22210

Figure Legends

Figure 1. Circadian rhythms of peptide content in somas and distal terminals of s-LNv neurons of intact living brains.

A. Dilp2-GFP images of s-LNv terminal projections into the dorsal protocerebrum (Z-projection stack) at ZT 2 and ZT 18. Scale bar = 25 µm.

B. Dilp2-GFP images of s-LNv somas at ZT2 and ZT23. Scale bar = 10 µm.

C. Terminal peptide content assessed at 5 time points in a 24 hour period in flies that were entrained 12h light:12h dark. n = 10-12 for all time points.

D. Somatic peptide content assessed at 5 time points over 24 hours in flies that were entrained 12h light:12h dark. n = 10-18 for each time point.

Figure 2. Circadian rhythms in neuropeptide release of s-LNv neuron terminals and somas.

A. FAP-based fluorescence increases upon release. Imaging shows greater release at terminals at ZT 3 than ZT 23 in entrained flies (12L:12D). Scale bar = 10 µm.

B. Quantification of neuropeptide release from terminals. n = 3-16.

C. Somatic neuropeptide release at ZT 3 and ZT 23 in entrained flies (12L:12D). Scale bar = 10 µm.

D. Quantification of neuropeptide release from somas. n = 10-18.

Figure 3. Tetanus Toxin (TetTx) attenuates release from s-LNv somas and terminals at their peak release times.

A. Release from s-LNv terminals at ZT 3 expressing tetanus toxin (n = 9) was 82% less than inactive mutant toxin controls (CON, n = 4). ***$p < 0.001$, unpaired t test.

B. Release from s-LNv somas at ZT 23 expressing tetanus toxin (n=12) was 69% less than controls (n = 8) expressing inactive mutant toxin. ***$p < 0.001$, unpaired t test.

Figure 4. Ca^{2+} source is different for neuropeptide release by s-LNv neuron somas and terminals.

A. Peak release (ZT 3) by terminals is inhibited by Cd^{2+} (10 µM, n = 13) compared to controls (n = 14). **p < 0.01, unpaired t test.
B. Somatic at peak release (ZT 23) is not affected by Cd^{2+} (10 µM, n = 13). For CON, n = 14). P = 0.8493, unpaired t test.
C. Peak release (ZT 3) by terminals is not different between Xestospongin C (20µM, n = 9) and control exposed terminals (CON, n = 16). p = 0.3126, unpaired t test.
D. Peak somatic release (ZT 23) is significantly reduced by Xestospongin C (20µM) (n = 16) compared to controls (CON, n = 21). *p < 0.05, unpaired t test.

Figure 5. IP3 sponge disrupts neuropeptide release from s-LNv somas and alters behavior.
A. Circadian rhythms in terminal neuropeptide release continued when IP_3 signaling was disrupted through expression of UAS-*IP3-sponge* in PDF cells. Note the difference between ZT 23 (n = 13) and ZT 3 (n = 13), p < 0.01, unpaired t test.
B. Circadian rhythms in somatic neuropeptide release was abolished when IP_3 was disrupted through expression of UAS-*IP3-sponge* in PDF cells. Note that there was no significant difference between ZT 23 (n=8) and ZT 3 (n = 7), p = 0.907, unpaired t test.
C. Expression of UAS-*IP3-sponge* using *Pdf*-Gal4 driver significantly reduced rhythmicity of fly locomotor behavior. One-way ANOVA revealed a statistically significant difference (p < 0.001). A post hoc comparison (Tukey's test) revealed differences in rhythmicity between UAS-*Dilp2-FAP*; UAS-*IP3 sponge*/*Pdf*-Gal4 (n=96, n = 4) and both genetic controls UAS-*IP3sponge/*+ (p < 0.01; n=88, n = 4) and UAS-*Dilp2-FAP*; *Pdf*-Gal4 (**p < 0.001; n=91, n = 4). There was no significant difference between the two control lines UAS-*IP3 sponge/*+ and UAS-*Dilp2-FAP*; *Pdf*-Gal4 (p = 0.176).
D. Expression of UAS-*IP3 sponge* using *Pdf*-Gal4 driver had no effect on period of rhythmic locomotor behavior. A one-way ANOVA revealed no significant difference (p = 0.607).

Figure S1. Neuropeptide content and release in l-LNv terminals and somas.
A. Neuropeptide content in l-LNv terminals. One-way ANOVA revealed no significant difference (p = 0.403) across the day.

B. Neuropeptide content in l-LNv cell bodies. A one-way ANOVA revealed no significant difference in content ($p < 0.536$) across the day.

Fig. S2. Circadian rhythms in neuropeptide release of l-LNv neuron terminals and somas.

A. Top, images of neuropeptide release by l-LNv nerve terminals at ZT3 and ZT 23 (scale bar = 10 µm). Bottom, neuropeptide release by l-LNv nerve terminals across the day and night. n = 8-13 for each point.

B. Top, images of neuropeptide release in l-LNv cell bodies during the morning (ZT3) and late night (ZT23). Scale bar =10 µm). Bottom, neuropeptide release by l-LNv somas across the day and night. n = 6-13 for each time point.

Fig. S3. Depolarization-evoked neuropeptide release at s-LNv terminals at ZT 1, when peptide content is high and endogenous release is low. For release measurements, the membrane impermeant MG derivative MG-B-Tau (MG) was used. Depolarization was evoked application of 70 mM K^+. Total Dilp2-Fap content was revealed by application of membrane permeant MGnBut (10 nM) for 1 hour. One-way ANOVA revealed a statistically significant difference ($p < 0.001$). Post hoc comparison (Tukey's test) revealed differences between MG and K^++MG ($p < 0.05$), MG and MGnBut (**$p<0.001$), and K^++MG and MGnBut ($p < 0.05$). MG n = 10, K^++MG n = 9, MGnBut n = 5.

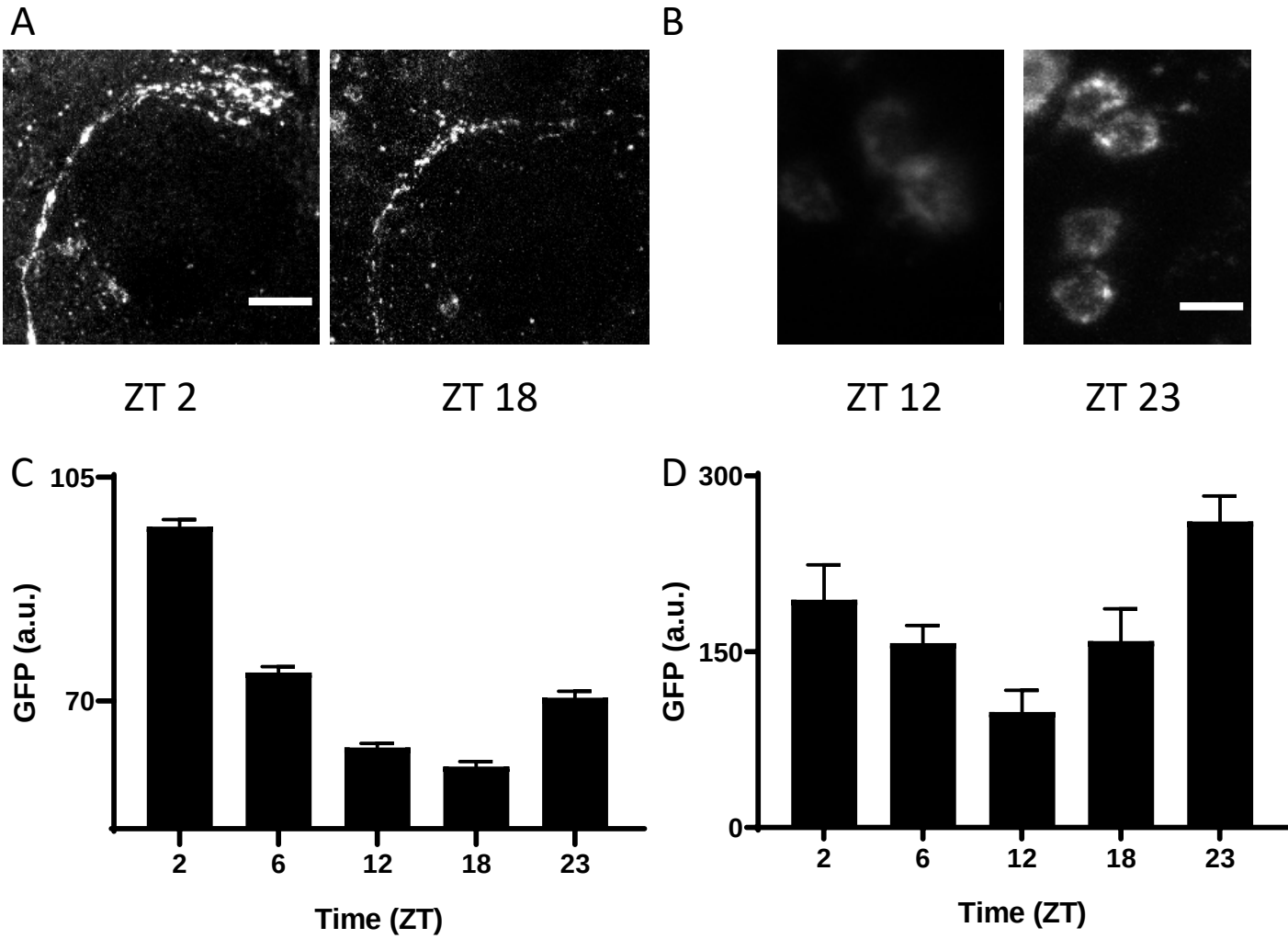
A
B
ZT 2
ZT 18
ZT 12
ZT 23
C
105
70
GFP (a.u.)
2
6
12
18
23
Time (ZT)
D
300
150
0
GFP (a.u.)
2
6
12
18
23
Time (ZT)

Figure 1

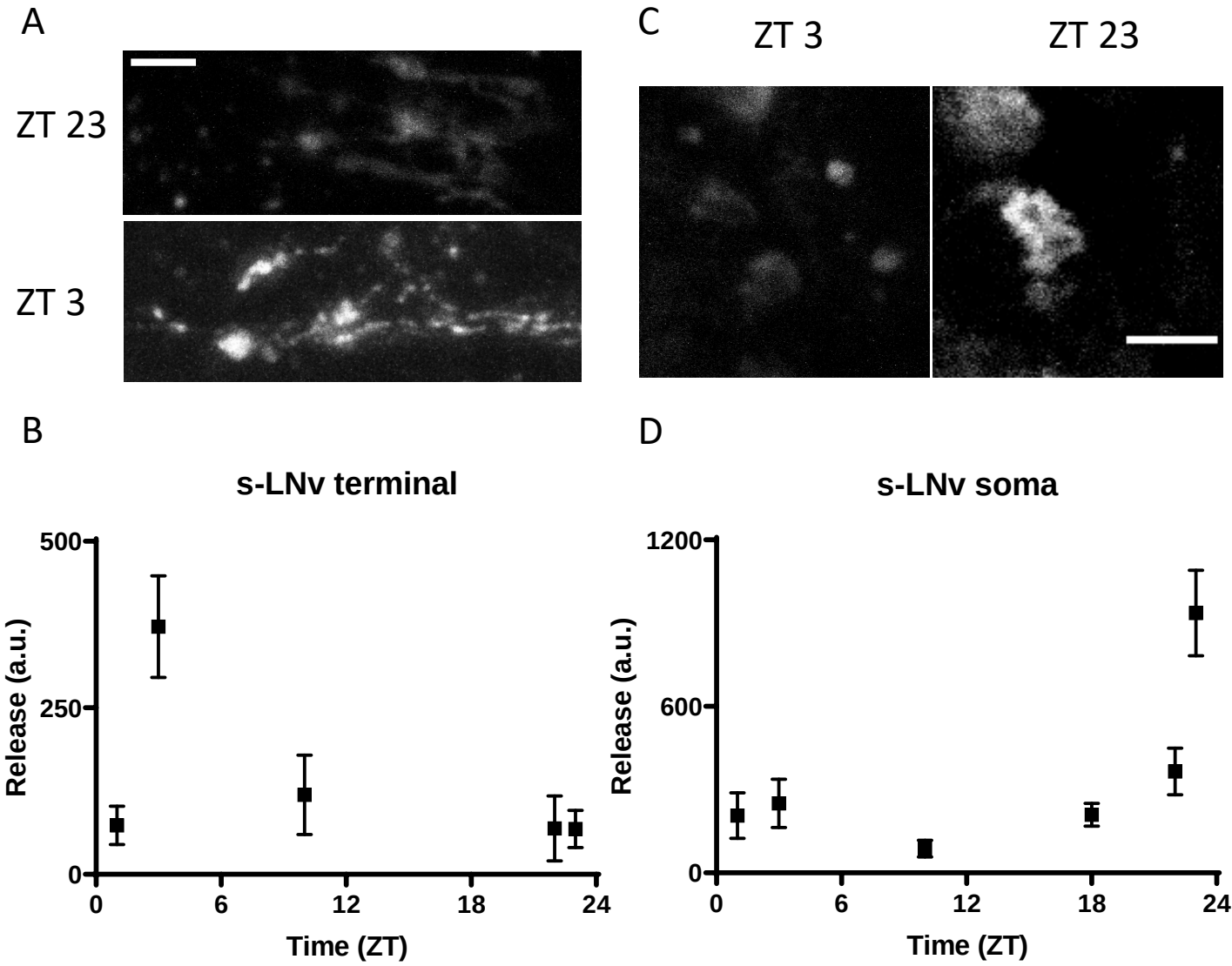
A
ZT 23
ZT 3
C
ZT 3
ZT 23
B
s-LNv terminal
Release (a.u.)
500
250
0
0
6
12
18
24
Time (ZT)
D
s-LNv soma
Release (a.u.)
1200
600
0
0
6
12
18
24
Time (ZT)

Figure 2

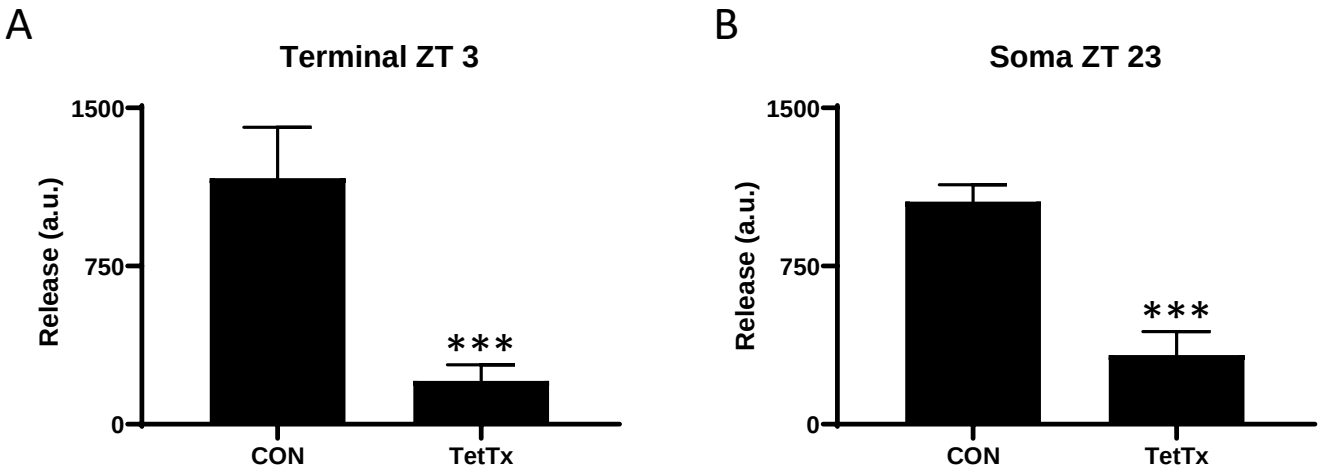
A
Terminal ZT 3
1500
750
0
Release (a.u.)
***
CON
TetTx
B
Soma ZT 23
1500
750
0
Release (a.u.)
***
CON
TetTx

Figure 3

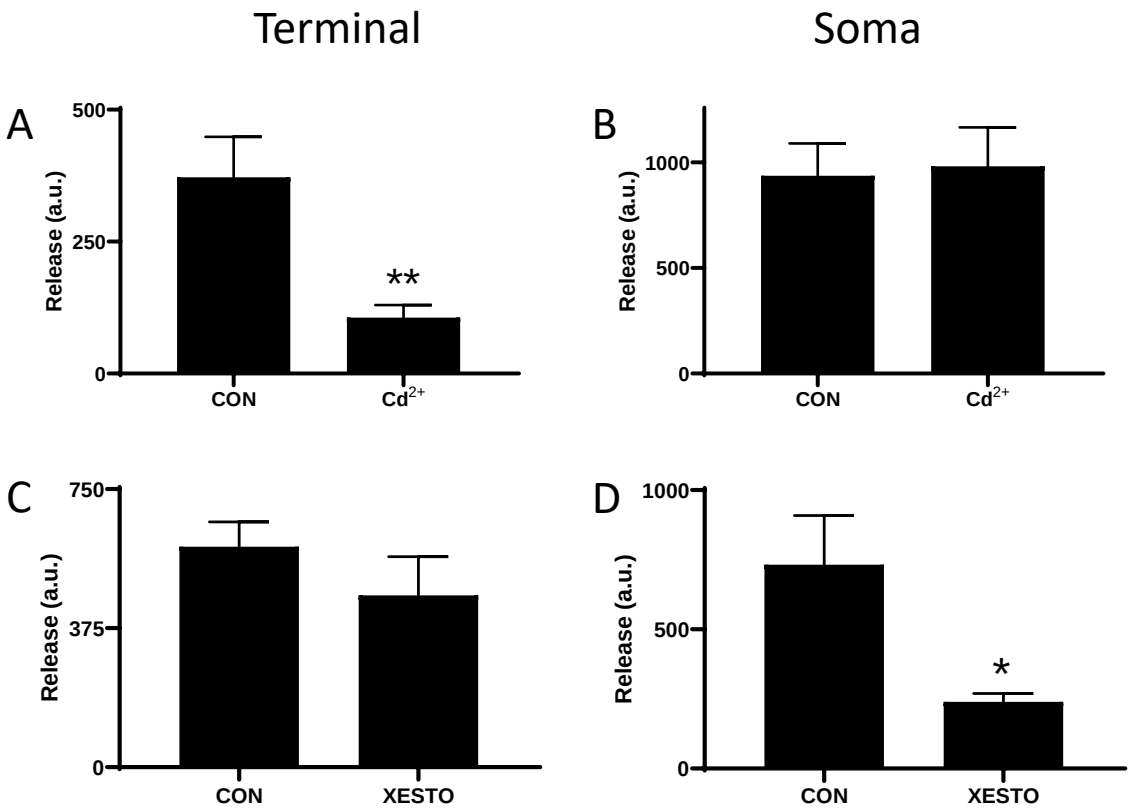
Terminal
Soma
A
B
C
D
Release (a.u.)
500
250
0
1000
500
0
750
375
0
1000
500
0
**
*
CON
Cd2+
CON
Cd2+
CON
XESTO
CON
XESTO

Figure 4

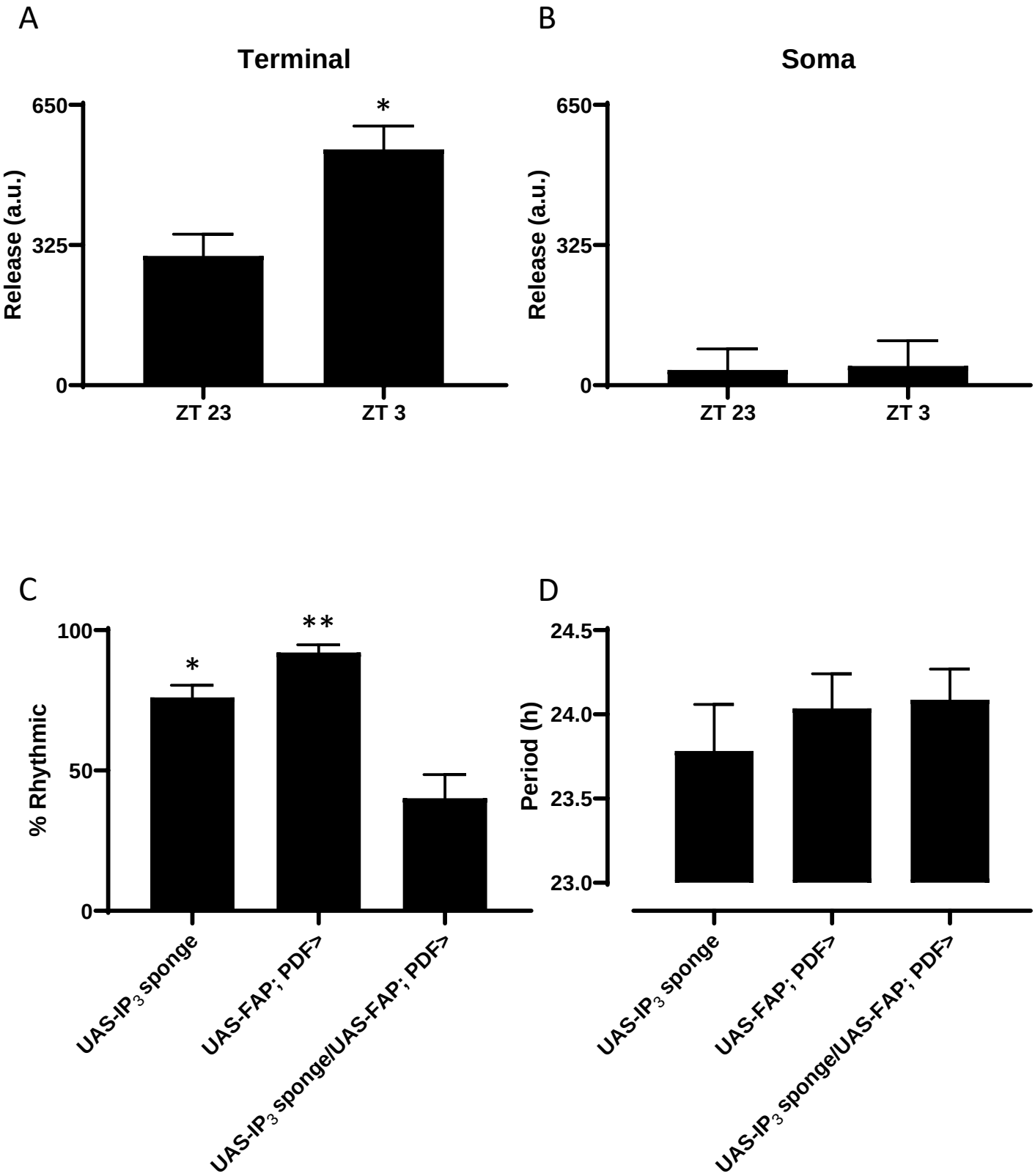
A
Terminal
650
325
0
Release (a.u.)
*
ZT 23
ZT 3
B
Soma
650
325
0
Release (a.u.)
ZT 23
ZT 3
C
100
50
0
% Rhythmic
*
**
UAS-IP3 sponge
UAS-FAP; PDF>
UAS-IP3 sponge/UAS-FAP; PDF>
D
24.5
24.0
23.5
23.0
Period (h)
UAS-IP3 sponge
UAS-FAP; PDF>
UAS-IP3 sponge/UAS-FAP; PDF>

Figure 5

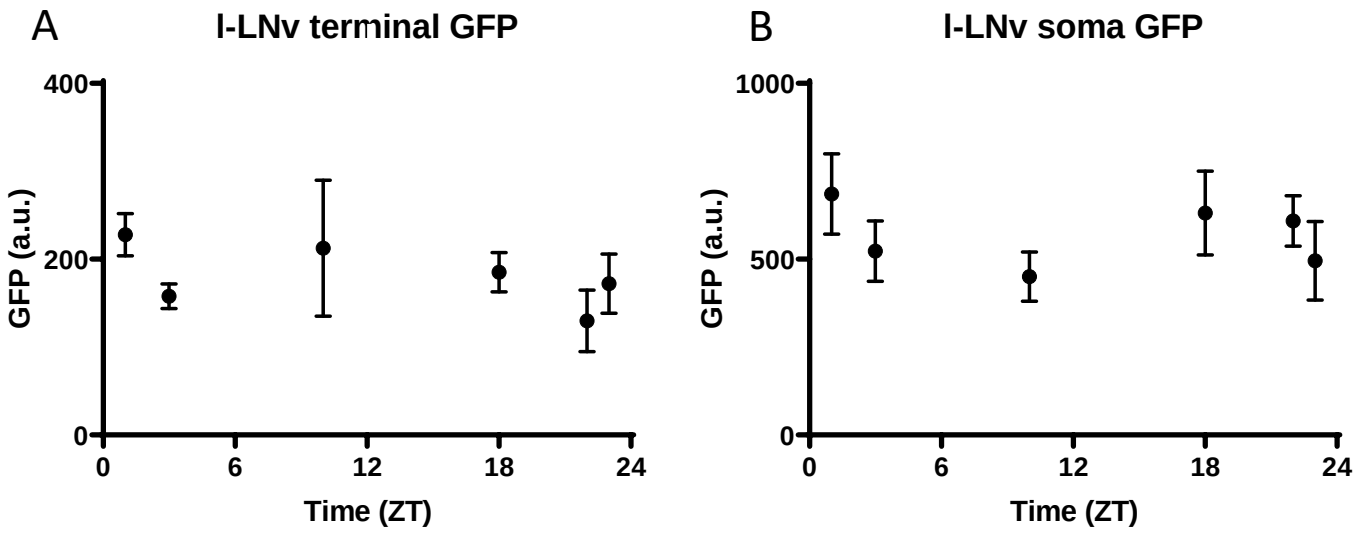
A
l-LNv terminal GFP
400
200
0
GFP (a.u.)
0
6
12
18
24
Time (ZT)
B
l-LNv soma GFP
1000
500
0
GFP (a.u.)
0
6
12
18
24
Time (ZT)

Figure S1

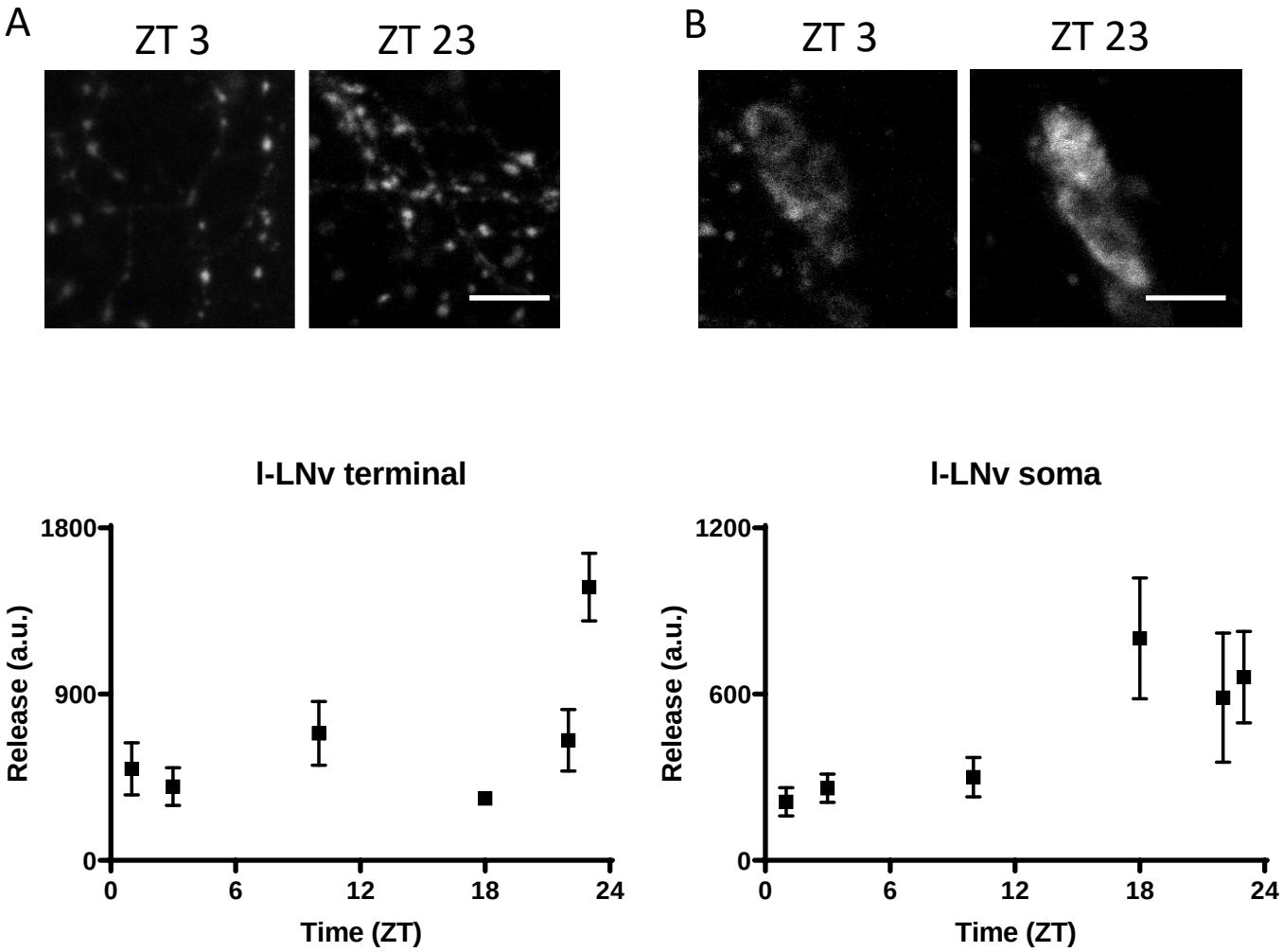
A
ZT 3
ZT 23
B
ZT 3
ZT 23
l-LNv terminal
Release (a.u.)
1800
900
0
0
6
12
18
24
Time (ZT)
l-LNv soma
Release (a.u.)
1200
600
0
0
6
12
18
24
Time (ZT)

Figure S2

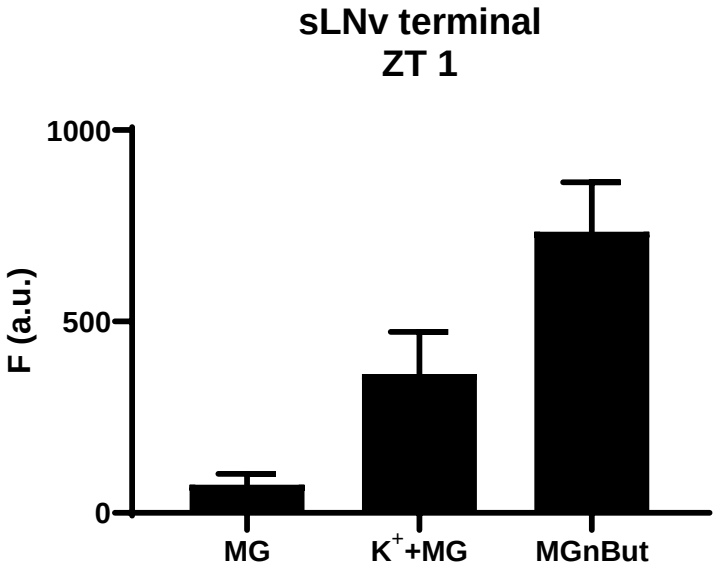

Figure S3